A model of enhanced electron concentration irregularities in the ionosphere: Perturbation amplitudes and hydrodynamic effects

C. Medina, V. Ríos* and E. Gómez
Universidad Nacional de Tucumán, Argentina
* *CONICET, Argentina*

RESUMEN

Se propone un modelo bidimensional para realizar simulaciones computacionales de irregularidades de concentración electrónica, en un rango extendido de altitud centrado en la base de la capa F, e incluyendo la dependencia de las frecuencias de colisiones y de recombinación, con la densidad. El modelo se prueba con diferentes amplitudes de perturbación en una franja limitada. Se encuentra que las amplitudes en un rango medio son más efectivas como efecto desestabilizante. Todos los resultados confirman la predicción de Rayleigh-Taylor hidrodinámica.

PALABRAS CLAVE: Ionósfera, irregularidades de concentración electrónica, inestabilidad de Rayleigh-Taylor, efecto hidrodinámico, amplitud de perturbación.

ABSTRACT

A bidimensional model is proposed to perform computer simulations of enhanced electron concentration irregularities, in an extended altitude range centered at the bottom of the F layer, and including the dependence of collision and recombination frequencies on density. The model is tested with different perturbation amplitudes in a limited fringe. We find that amplitudes in a medium range are more effective as a destabilising effect. All results confirm the hydrodynamic Rayleigh-Taylor prediction.

KEY WORDS: Ionosphere, electron concentration irregularities, Rayleigh-Taylor instability, hydrodynamic effect, perturbation amplitude.

INTRODUCTION

Generalized Rayleigh-Taylor (R-T) instability plays a predominant role in the evolution of long-wavelength irregularities in the ionosphere (Ossakow *et al.*, 1979; Zalesak *et al.*, 1982). This instability requires a seeding process provided by gravity waves producing density modulations at the bottom of the F layer (Kelley and Hysell, 1991; Huang *et al.*, 1993; Singh *et al.*, 1997).

The two-fluid model assumed in R-T instability implies alternately depleted and enhanced electron concentration regions (Keskinen *et al.*, 1980; Keskinen *et al.*, 1981). Their morphology and altitude location have not always confirmed theoretical predictions. In particular, an enhanced density region should sink into a lighter medium below, as predicted by hydrodynamic R-T (Kelley, 1989).

In this paper, a bidimensional model, including dependence of collision frequency and recombination rate on density, is shown to predict the enhanced electron concentration irregularities for different values of perturbation amplitude.

THE MODEL

We use a standard electron density profile approached by steps through exponential functions, $n_0(y)$ (Figure 1).

The perturbed profile is

$$n_0(x,y) = n_0(y)\left\{1 + A_0 \cos(kx)C(y)\right\}, \qquad (1)$$

where the second term on the right hand side bracket represents a perturbation with amplitude A_0; x is the east-west direction (surface waves); k is the perturbation wave number; and $C(y)$ is a limited altitude fringe.

The constants A_0 and k depend on the amplitude and wave number of the perturbing gravity wave. We assume values of $A_0 = 0.01, 0.05,$ and 0.1 corresponding to perturbation amplitudes of 1%, 5%, and 10%, respectively; and $k = 6.28 \cdot 10^{-4}$ m^{-1} corresponding to a 10 km wavelength. We consider only the horizontal east-west direction for the wave-like perturbation, since it is dominant (Kelley, 1989; Huang *et al.*, 1993; Singh *et al.*, 1997).
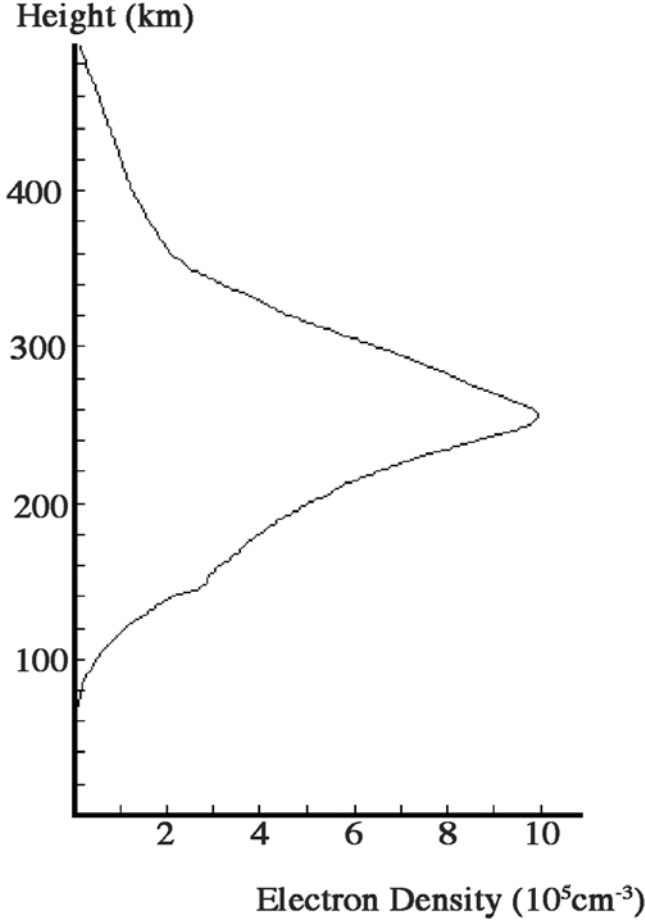
Height (km)

Fig. 1. Electron Density Profile.

The limited altitude fringe, $C(y)$, allows a better convergence in numerical computation and is consistent with the fact that gravity waves are more effective in creating density modulations at the bottom of the F layer (Tsunoda and White, 1981; Tsunoda 1983; Kelley, 1989; Singh *et al.*, 1997). We assume a 100 km thick fringe, centered at 250 km altitude. Thicker fringes produce more perturbed profiles at transient times (not shown here).

We have

$$C(y) = \begin{cases} (y - y_l)/(y_b - y_l), & y_l \leq y \leq y_b \\ (y_m - y)/(y_m - y_1), & y_b \leq y \leq y_m \\ 0, & y \leq y_l \ \ or \ \ y \geq y_m \end{cases} \quad (2)$$

where y_l, and y_m stand for the lower and upper limits of the fringe, and y_b is the elevation of the F layer bottom.

The fluid equations can be written (Uman, 1964):

$$\frac{\partial n}{\partial t} + \nabla \cdot (n_\alpha V_\alpha) = -v_R(n_\alpha - n_{\alpha 0}) \quad (3)$$

$$0 = -k_B T_e \nabla n_e - e n_e \left(-\nabla \phi + V \times B + E_0\right) \quad (4)$$

$$m_i n_i \left(\frac{\partial}{\partial t} + V_i \cdot \nabla\right) V_i = -k_B T_i \nabla n_i - e n_i \left(-\nabla \phi + V_i \times B + E_0\right) + m_i n_i g - m_i n_i v_{in} V_i \quad (5)$$

$$\nabla \cdot J = 0 \quad (6)$$

$$J = e\left(n_i V_i - n_e V_e\right), \quad (7)$$

where α refers to electrons (e) or ions (i), and n, v_{in}, v_R, k_B, ϕ, V, B, E_0, m, e, g, J, are respectively the density, collision frequency, recombination rate, Boltzmann constant, electrostatic potential, velocity, magnetic field, zero order electric field, mass, electron charge, gravity, and current density. The total electric field is $E = E_0 - \mathbf{grad}\ \phi$. We assume E_0 directed westward in the x direction; g is downward (-y direction); and B is to the north (z direction).

We assume quasineutrality ($n_e \approx n_i \approx n$). Inertial and pressure effects are ignored (Keskinen *et al.*, 1981). If $\mathbf{grad}\ \phi = \mathbf{grad}\ \phi_1 + mg/e$ (Ossakow *et al.*, 1979), and solving (4) and (5) for the velocities, the system becomes

$$\frac{\partial n}{\partial t} - \frac{1}{B}(\nabla_\perp \phi_1 \times e_z) \cdot \nabla_\perp n = -v_R(n - n_0) \quad (8)$$

$$\nabla_\perp \cdot (v_{in} n \nabla_\perp \phi_1) = B(g \times e_z) \cdot \nabla_\perp n + E_0 \cdot \nabla_\perp (v_{in} n). \quad (9)$$

Since v_{in} and v_R are both proportional to n (Rishbeth and Garriot, 1969), we may set

$$v_{in} = k_{in} n \quad (10)$$

$$v_R = k_R n, \quad (11)$$

where $k_{in} = 1 \cdot 10^{-10} \text{ s}^{-1} \text{ cm}^3$ and $k_R = 2 \cdot 10^{-9} \text{ s}^{-1} \text{ cm}^3$, to match the values of the maximum concentration level proposed by Zalesak *et al.* (1982). Thus, (8) and (9) become

$$\frac{\partial n}{\partial t} - \frac{1}{B}(\phi_y n_x - \phi_x n_y) + k_R n(n - n_0) = 0 \quad (12)$$

$$(k_{in} n^2 \phi_x)_x + (k_{in} n^2 \phi_y)_y + B n_x (g - 2k_{in} V_d n) = 0, \quad (13)$$

where the subscripts x and y denote differentiation $\partial/\partial x$ and $\partial/\partial y$, and V_d is the drift velocity, $V_d = E_0/B$. We assume $V_d = 20 \text{ m s}^{-1}$, directed downward.

The software PDE2D (Sewell, 1985), based on the finite element method, was used to solve the system. The element sizes were scaled according to electron concentration.

We used fixed boundary conditions at the bottom and the top of the integration region, assuming that n and ϕ remain unaffected far from the bottom of the F layer. For the sides of the region, we used free (Gibbs) boundary conditions as follows:

$$-\frac{1}{B}n\phi_y e_x + \frac{1}{B}n\phi_x e_y = 0 \tag{14}$$

$$k_{in}n^2\phi_x e_x + k_{in}n^2\phi_y e_y = 0 , \tag{15}$$

where e_x and e_y are versors in the x and y directions. Equation (14) holds because it is a sum of scalar products of perpendiculars vectors, while (15) implies that n varies only with altitude.

RESULTS AND DISCUSSION

Figures 2, 3, and 4 represent the evolution at 1 minute intervals (*a, b, c, d*) for perturbations of amplitude $A_0 = 1\%$, 5%, and 10%, respectively. Contours are drawn at 10^5 cm^{-3} intervals for Figures *a, b, c*, and at $2 \cdot 10^5$ for Figures *d*.
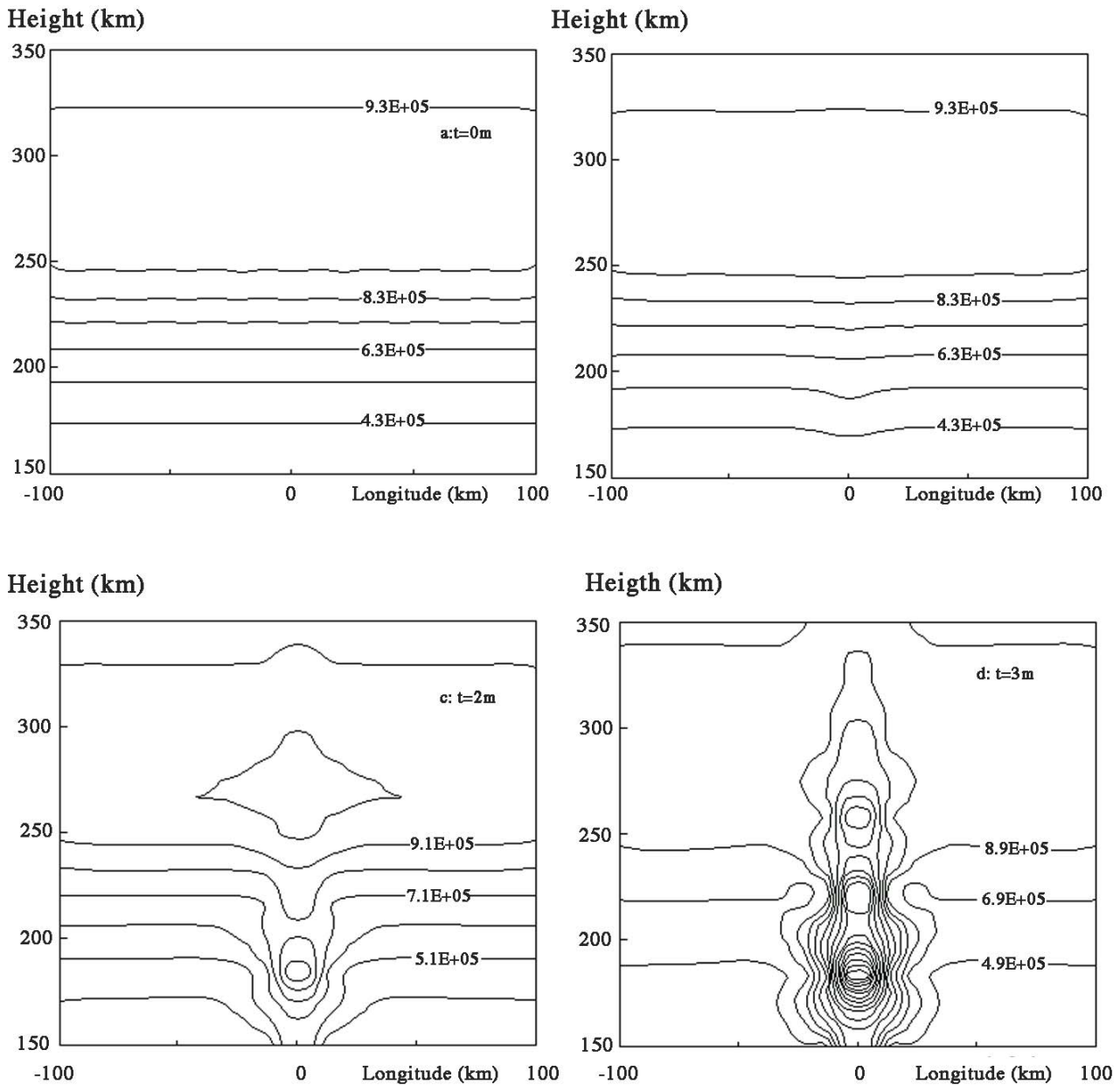
Perturbation amplitude: 1%.

Fig. 2. *a, b, c*, and *d*, representing isodensity contour sketches at 0, 1 , 2, and 3 minutes, respectively.
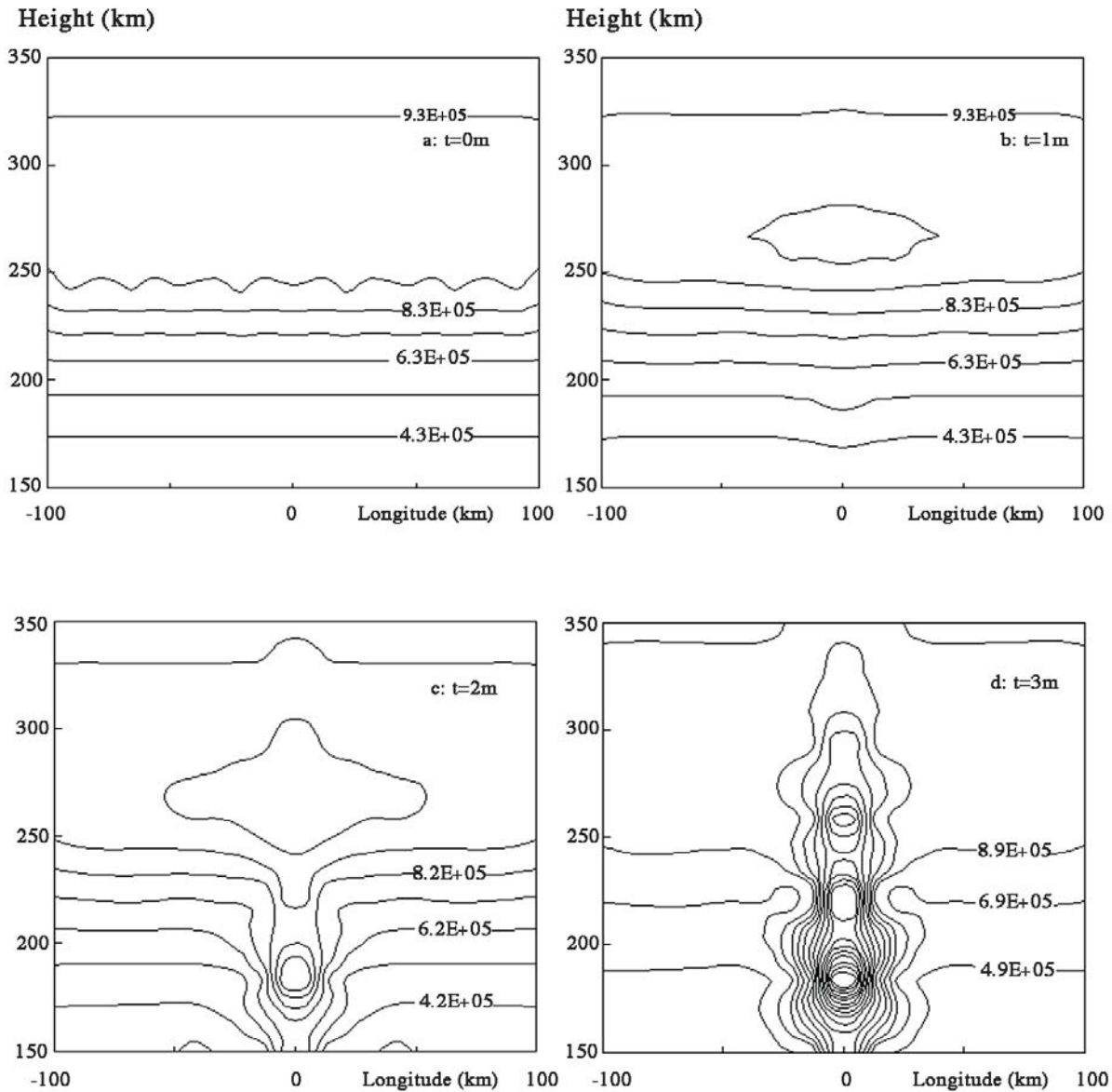
Perturbation amplitude: 5%.

Fig. 3. *a, b, c*, and *d*, representing isodensity contour sketches at 0, 1 , 2, and 3 minutes, respectively.

Figures *d* show a well developed irregularity. Density gradients are stronger in Figure 3 ($A_0 = 5\%$). The fact that density gradients decrease at lower and higher perturbation amplitudes shows that there is a preferred range of perturbation amplitude for the instability to be more effective in irregularity generation. As one might expect, a 5% perturbation amplitude is more effective than a 1% one. An amplitude of 10% is less effective than one of 5% because large perturbations alter the density profile (Figure 4a) which prevents the seeding process (Medina, 2000).

Figures *c* and *d* show that the hydrodynamic R-T appears to hold, since irregularities drop to levels below that of

maximum concentration as if a heavy fluid were dropping into a lighter one.

In situ as well as ground based measurements agree with these results. Using Radon transform of ionospheric delays from NNSS satellite signals at sequenced angles in Tucumán, Soria (1999) detected field aligned overdense patches below the F_2 peak, which were large at the bottom and constricted toward the top. From Atmosphere Explorer E satellite data, Singh *et al.* (1997) report enhanced density regions moving downward. From San Marco and Dynamics Explorer B satellite data, Hanson (1990) found overdense plasma regions below the F2 peak, and downward veloci-
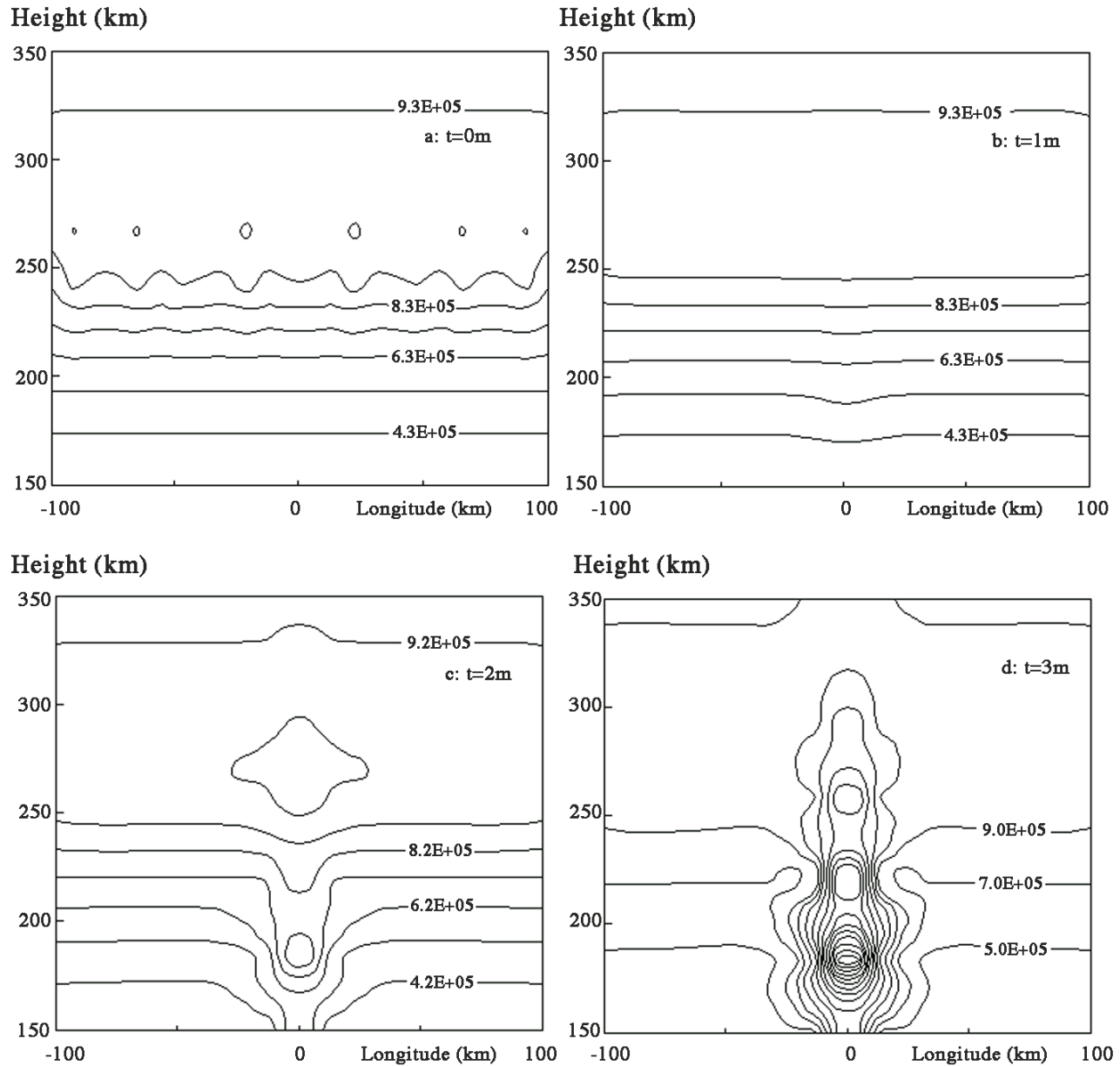
Perturbation amplitude: 10%.

Fig. 4. *a, b, c,* and *d,* representing isodensity contour sketches at 0, 1 , 2, and 3 minutes, respectively.

ties in the more structured bubble edges. Fukao *et al.* (1990), using MU Radar, observed field-aligned irregularities presenting downward velocities about midnight.

However, overdense regions often appear rather stable. Some observations can be ascribed to a different type of process, e.g., bottomside sinusoidal structures (BSS), which present different properties from R-T generated irregularities (Valladares *et al.*, 1983; Cragin *et al.*, 1985; Basu *et al.*, 1986). Further research on time behaviour, and a larger range of gravity wavelengths, would be needed to confirm a connection between both types of irregularities.

BIBLIOGRAPHY

AKASOFU, S. and S. CHAPMAN, 1972. Solar Terrestrial Physics, Oxford University Press, UK.

BASU, S., S. BASU, C. VALLADARES, A. DASGUPTA and H. WHITNEY, 1986. Scintillations associated with bottomside sinusoidal irregularities in the equatorial F region. *J. Geophys. Res., 91*, 270-276.

CRAGIN, B., W. HANSON, J. MCCLURE and C. VALLADARES, 1985. Bottomside sinusoidal irregu-

larities in the equatorial F region. II - Cross-correlation and spectral analysis. *J. Geophys. Res., 90,* 1721-1734.

FUKAO, S., M. KELLEY, M. YAMAMOTO, T. TAKAMI, T. TSUDA and S. KATO, 1990. Mid-latitude F region field aligned irregularities observed by the 50 MHz MU Radar, Conference Digest of Eight International Symposium on Equatorial Aeronomy, 167.

HANSON, W., 1990. Equatorial irregularities as viewed from satellites, Conference Digest of Eight International Symposium on Equatorial Aeronomy, 175.

HUANG, C., M. KELLEY and D. HYSELL, 1993. Nonlinear Rayleigh-Taylor instabilities, atmospheric gravity waves and equatorial spread-F. *J. Geophys. Res., 98, 45,* 15631-15642.

KELLEY, M., 1989. The Earth's Ionosphere, Academic, San Diego, California.

KELLEY, M. and D. HYSELL, 1991. Equatorial spread-F and neutral atmospheric turbulence: a review and a comparative anatomy. *J. Atmos. Terr. Phys., 53,* 695.

KESKINEN, M., S. OSSAKOW and P. CHATURVEDI, 1980. Preliminary report of numerical simulations of intermediate wavelength collisional Rayleigh-Taylor instability in Equatorial Spread F. *J. Geophys. Res., 85,* A4, 1775-1778.

KESKINEN, M., E. SZUSZCZEWICZ, S. OSSAKOW and J. HOLMES, 1981. Nonlinear theory of experimental observations of the local collisional Rayleigh-Taylor instability in a descending equatorial Spread-F ionosphere, *J. Geophys. Res., 86,* A7, 5785.

MEDINA, C., 2000. Irregularidades de concentración electrónica en la ionósfera superior, internal publication, UNT, Tucumán, Argentina.

OSSAKOW, S., S. ZALESAK, B. MCDONALD and P. CHATURVEDI, 1979. Nonlinear equatorial spread F, dependence on altitude of F peak and bottomside back-ground electron density gradient scale length. *J. Geophys. Res., 84*, 17.

RISHBETH, H. and O. GARRIOT, 1969. Introduction to Ionospheric Physics, Academic Press Inc., New York.

SEWELL, G., 1085. Analysis of a finite element method: PDE/PROTRAN, Springer Verlag.

SINGH, S., F. JOHNSON and R. POWER, 1997. Gravity wave seeding of equatorial plasma bubbles. *J. Geophys. Res., 102,* 7399-7410.

SORIA, F., 1999. Tomografía Ionosférica, internal publication, UNT, Tucumán, Argentina.

TSUNODA, R., 1983. On the generation and growth of equatorial backscatter plumes, 2, Structuring of the west walls of upwellings. *J. Geophys. Res., 88,* 4869-4874.

TSUNODA, R. and B. WHITE, 1981. On the generation and growth of equatorial backscatter plumes, 1, Wave structure in the bottomside F layer. *J. Geophys. Res., 86,* 3610-3616.

UMAN M., 1964. Introduction to Plasma Physics, McGraw-Hill Inc., New York.

VALLADARES, C., W. HANSON, J. MCCLURE and B. CRAGIN, 1983. Bottomside sinusoidal irregularities in the equatorial F region. *J. Geophys. Res., 88,* 8025-8042.

ZALESAK, S., S. OSSAKOW and P. CHATURVEDI, 1982. Nonlinear equatorial spread-F: effect of neutral wind and background Pedersen conductivity. *J. Geophys. Res., 87,* 151-166.

_____

C. Medina, V. Ríos[*] and E. Gómez
Universidad Nacional de Tucumán, Argentina
[*] *CONICET, Argentina*
Email: CFMedina@herrera.unt.edu.ar